Culture on Tissue-Specific Coatings Derived from α-Amylase-Digested Decellularized Adipose Tissue Enhances the Proliferation and Adipogenic Differentiation of Human Adipose-Derived Stromal Cells

Arthi Shridhar, Alan Y. L. Lam, Yu Sun, Craig A. Simmons, Elizabeth R. Gillies, and Lauren E. Flynn*

While extracellular matrix (ECM)-derived coatings have the potential to direct the response of cell populations in culture, there is a need to investigate the effects of ECM sourcing and processing on substrate bioactivity. To develop improved cell culture models for studying adipogenesis, the current study examines the proliferation and adipogenic differentiation of human adipose-derived stem/stromal cells (ASCs) on a range of ECM-derived coatings. Human decellularized adipose tissue (DAT) and commercially available bovine tendon collagen (COL) are digested with α-amylase or pepsin to prepare the coatings. Physical characterization demonstrates that α-amylase digestion generates softer, thicker, and more stable coatings, with a fibrous tissue-like ultrastructure that is lost in the pepsin-digested thin films. ASCs cultured on the α-amylase-digested ECM have a more spindle-shaped morphology, and proliferation is significantly enhanced on the α-amylase-digested DAT coatings. Further, the α-amylase-digested DAT provides a more pro-adipogenic microenvironment, based on higher levels of adipogenic gene expression, glycerol-3-phosphate dehydrogenase (GPDH) enzyme activity, and perilipin staining. Overall, this study supports α-amylase digestion as a new approach for generating bioactive ECM-derived coatings, and demonstrates tissue-specific bioactivity using adipose-derived ECM to enhance ASC proliferation and adipogenic differentiation.

1. Introduction

The extracellular matrix (ECM) is a dynamic network of proteins, glycoproteins, and polysaccharides, with tissue-specific composition and ultrastructure.[1,2] Despite the recognized importance of the ECM in directing cellular processes, the majority of in vitro cell biology studies are performed on rigid 2D tissue culture plastic (TCP) substrates.[3,4] These systems are convenient for downstream analyses,[5] but lack the complexity of the native cellular milieu. To incorporate cell–ECM interactions within these platforms, TCP is often coated with purified ECM components (e.g., collagens, laminin, or fibronectin), which have been shown to mediate cell behavior.[6–8] However, these simplified models lack the complex ultrastructure and biochemical composition of the native ECM, which may limit the translatability of the findings from in vitro to in vivo systems.

In general, there is a need to develop higher-fidelity culture models within TCP formats that more closely approximate the tissue-specific ECM microenvironment, while remaining readily characterizable using standard biological assays. The method of tissue decellularization is a

Dr. A. Shridhar, Prof. E. R. Gillies, Prof. L. E. Flynn
Department of Chemical and Biochemical Engineering
Thompson Engineering Building
The University of Western Ontario
London N6A 5B9, Ontario, Canada
E-mail: lauren.flynn@uwo.ca

A. Y. L. Lam, Prof. Y. Sun, Prof. C. A. Simmons
Institute of Biomaterials and Biomedical Engineering
University of Toronto
Toronto M5S 3G9, Ontario, Canada

Prof. Y. Sun, Prof. C. A. Simmons
Department of Mechanical and Industrial Engineering
University of Toronto
Toronto M5S 3G8, Ontario, Canada

Prof. E. R. Gillies
Department of Chemistry
The University of Western Ontario
London N6A 5B7, Ontario, Canada

Prof. L. E. Flynn
Department of Anatomy & Cell Biology
Schulich School of Medicine & Dentistry
The University of Western Ontario
London N6A 3K7, Ontario, Canada

**ADVANCED
SCIENCE NEWS**
www.advancedsciencenews.com

**Biotechnology
Journal**
www.biotechnology-journal.com

useful approach for isolating tissue-specific ECM for bioscaffold fabrication.[9–13] To generate coatings, decellularized tissues are typically digested using the proteolytic enzyme pepsin.[14–17] However, pepsin digestion is highly nonspecific, with digestion times and enzyme activity influencing the profile of resulting peptides.[14] Further, it remains unclear whether pepsin digestion is the best approach for preserving ECM bioactivity. Some studies indicate that pepsin-digested ECM coatings promote cell proliferation and/or differentiation compared to collagen type I,[17] gelatin,[15] Matrigel,[18] and uncoated substrates.[17] Conversely, others have suggested that they provided no benefit relative to collagen type I-coated and uncoated TCP.[16,19] Notably, biomaterials fabricated with pepsin-digested ECM have been reported to have low stability unless chemically crosslinked,[20,21] likely due to the fragmented nature of the digested ECM. These findings suggest that pepsin-digested ECM bioactivity may be highly dependent on the specific ECM sources used, cell types under investigation and culture conditions.

As an alternative to pepsin, our group has established protocols using enzymatic digestion with α-amylase to generate porous foams and microcarriers derived from decellularized tissues.[22–25] Digestion with α-amylase enhances collagen fibril dispersion in acetic acid by destabilizing collagen-glycoprotein complexes[26] and cleaving carbohydrate groups in the telopeptide regions of the collagen, leaving peptide bonds unaltered to better preserve the complex protein-rich network of the ECM.[27] Although α-amylase-digested ECM-derived bioscaffolds have been shown to modulate the proliferation and differentiation of human adipose-derived stem/stromal cells (ASCs) in culture,[23–25] their bioactivity relative to substrates prepared with pepsin-digested ECM remains unexplored.

With the goal of developing improved culture models for studying adipogenesis, the current study compared the proliferation and adipogenic differentiation of human ASCs cultured on α-amylase-digested fibrous coatings to pepsin-digested thin films and uncoated TCP controls. Human decellularized adipose tissue (DAT) and commercially available bovine tendon collagen (COL) were explored as ECM sources to assess potential tissue-specific effects on the cellular response. We hypothesized that ASC attachment, proliferation, and adipogenesis would be enhanced on the coatings derived from tissue-specific ECM (i.e., DAT), with the bioactivity of the ECM better conserved through digestion with the glycolytic enzyme α-amylase as compared to the proteolytic enzyme pepsin.

2. Experimental Section

2.1. Materials

Unless otherwise specified, all chemicals and reagents were purchased from Sigma Aldrich and used as received.

2.2. Adipose Tissue Procurement and Processing

Subcutaneous adipose tissue was collected from elective lipo-reduction surgeries at the London Health Sciences Centre in London, ON, Canada (HREB# 105426). The tissue was processed using published methods for ASC isolation[28] or decellularization[13] within 2 h. Isolated ASCs were cultured in proliferation medium (DMEM:Ham's F-12 supplemented with 10% fetal bovine serum (FBS), 100 U mL^{-1} penicillin, and 0.1 mg mL^{-1} streptomycin (pen-strep)). Passage 2 (P2) ASCs were used for all seeding and characterization experiments. ASC immunophenotype was confirmed prior to seeding using a Guava easyCyte 8HT flow cytometer (Millipore, Billerica, MA, USA)[29] (Table S1, Supporting Information).

2.3. Enzyme Digestion and Coating Preparation

Human DAT pooled from five donors and bovine tendon collagen (COL) (Sigma, Cat #: 9007345, Product #: C9879) were cryo-milled using published methods[30] and decontaminated in 70% ethanol overnight, followed by PBS rinsing. α-amylase-digested DAT and COL suspensions (25 mg mL^{-1}) were synthesized using established protocols and stored at 4 °C.[24] Pepsin-digested ECM solutions (25 mg mL^{-1}) were prepared using published protocols in 0.2 M acetic acid.[31] The resulting solutions were neutralized with 5.7 N NaOH to inactivate the enzyme, centrifuged at 12 000 × g and the supernatant filtered through a 0.22 µm syringe filter (Millipore). The final ECM solutions were stored at 4 °C, for a maximum of 2 months.

For scanning electron microscopy (SEM) and coating thickness measurement studies, 8 mm round glass coverslips were positioned at the bottom of 12-well TCP plates. For mechanical testing and immunohistochemical characterization studies, 25 mm square glass coverslips were positioned at the bottom of 6-well TCP plates. For all other studies, 12-well TCP plates were coated directly. To generate the coatings, 12-well or 6-well TCP plates were coated with 0.6 mL or 1.2 mL per well of enzyme-digested ECM, respectively, and the plates were left to dry overnight in a biological safety cabinet.

2.4. Physical Characterization of Coating Materials

2.4.1. SDS-PAGE Analysis of ECM Digests

For SDS-PAGE analysis, 20 µL volumes of the digested samples (diluted to 1 mg mL^{-1} in 0.2 M acetic acid based on starting ECM mass) were run on Tris-HCl, 6–20% gradient polyacrylamide gels in running buffer comprised of 25 mM Tris, 1% glycine, and 0.1% SDS. Gel electrophoresis (Bio-Rad, USA, Mini-PROTEAN Tetra vertical electrophoresis cell) was performed in comparison to a BLUeye pre-stained broad size range protein standard (Cat #: PM0070500) and visualized with Gel Code Blue Protein Stain (Thermo Scientific).

2.4.2. SEM Analysis of Coating Ultrastructure

SEM was used to visualize the ultrastructure of the DAT and COL coatings prior to seeding using established protocols.[23] α-amylase DAT and COL samples were scratched with a scalpel blade to visualize the interior structure.

2.4.3. Toluidine Blue Staining

Toluidine blue staining was performed using published protocols to qualitatively assess the DAT and COL coatings before and after two rinses with proliferation medium used in preparation for the cell culture studies.[15] Uncoated wells were included as a control. The samples were visualized at 10× magnification using an EVOS XL CORE bright field microscope (Life Technologies).

2.4.4. Hydroxyproline Assay

The hydroxyproline assay was performed to provide a quantitative assessment of coating stability following rinsing. DAT and COL coating samples before and after two rinses in proliferation medium ($n = 3$ per group) were processed and evaluated using previously published methods.[32]

2.4.5. Coating Thickness

To assess the thickness of the α-amylase-digested coatings, the samples ($n = 3$ per group) were rinsed twice in PBS, scratched through the center with a scalpel blade and imaged from the side using a stereomicroscope. Approximately six nonoverlapping images were obtained across the scratched coating and the thickness was measured using ImageJ software.

A scratch test was performed in pepsin-digested coatings before and after two rinses in proliferation medium, followed by surface thickness evaluation using a mechanical stylus surface profiler (KLA Tencor P-10 Surface Profiler, Surface Science Western) ($n = 3$ per group). The scratch was made at the center of the coating, and three line scans at different regions were taken with six to seven randomly chosen readings within each scan used to estimate the average thickness of the coatings.

2.4.6. Mechanical Characterization Using Atomic Force Microscopy

Young's moduli (E) of the ECM coatings after the rinse step were determined in their hydrated states using an atomic force microscope (Bioscope Catalyst, Bruker). Samples were indented using the contact mode in fluid setting utilizing silicon nitride AFM cantilevers (Bruker, MLCT-O10 cantilever D) with an attached 5 μm radius spherical polystyrene bead. The cantilevers had a nominal spring constant of 0.03 N m^{-1} and precise spring constants were calibrated using the thermal tune method as per manufacturer instructions. Force-extension indentation curves were sampled to estimate Young's moduli with a force trigger of 4 nN prescribing the point at which the cantilever approach was stopped and then retracted.[33] Three replicates for the pepsin-digested samples and six replicates for the α-amylase-digested samples were evaluated, with six experimental points measured across each replicate to account for regional variability. The Hertz contact model for a spherical tip was applied to fit the rising slopes of the approach curve before relaxation using the Bruker NanoScope Analysis software, with conditions kept consistent between all samples and groups.[33] To eliminate possible stiffness effects of the underlying substrate, the indentation depth of each run was extrapolated and ensured to be ≤10% of the sample thickness.[34,35]

2.5. ASC Proliferation Studies

2.5.1. ASC Seeding and Culture

The coatings were rinsed twice in proliferation medium, and P2 ASCs were seeded at a density of 5000 cells cm^{-2} (37 °C, 5% CO_2). Uncoated coverslips were included as controls. Fresh proliferation medium was provided to all samples every 2–3 d.

2.5.2. Immunocytochemical Assessment of Cell Morphology and Proliferation

To assess cell attachment, morphology, and proliferation over time, immunocytochemical staining of vimentin with DAPI counter-staining was performed at 4 h, 24 h, 72 h, 7 d, and 14 d ($n = 3$ samples per group per trial, $N = 2$ trials with different ASC donors). At each timepoint, triplicate samples were fixed overnight in buffered 4% paraformaldehyde solution (pH 7.4) at 4 °C, rinsed in PBS, and blocked for 1 h (Tris buffered saline [TBS, pH 7.4], 1% BSA, 0.01% Triton X-100). Next, the samples were incubated overnight at 4 °C with rabbit monoclonal anti-vimentin (ab92547, Abcam, 1:200). The coatings were then rinsed in TBS before incubation with an Alexa Fluor 594 conjugated goat anti-rabbit IgG secondary antibody (ab150080, Abcam, 1:200) for 1 h at room temperature. Finally, the coatings were rinsed in PBS and mounted in Fluoroshield mounting medium (Abcam) with DAPI to visualize cell nuclei. Approximately ten nonoverlapping images were captured across each coating using an EVOS FL fluorescence imaging system. Nuclei per mm^2 were quantified under a single blind setup using ImageJ software.

2.6. ASC Differentiation Studies

2.6.1. ASC Seeding and Culture

The coatings were rinsed twice in proliferation medium and P2 ASCs were seeded at a density of 50 000 cells cm^{-2} in proliferation medium (37 °C, 5% CO_2).[30] Uncoated wells/coverslips were included as controls. Following a 24 h incubation to facilitate cell attachment, the samples were rinsed with PBS and cultured in serum-free adipogenic differentiation medium comprised of DMEM:Ham's F12 nutrient mixture supplemented with 33 μM biotin, 17 μM pantothenate, 66 nM human insulin, 1 nM tri-iodothyronine (T3), 10 μg mL^{-1} transferrin, 100 nM hydrocortisone, 100 U mL^{-1} penicillin, and 0.1 mg mL^{-1} streptomycin.[36] The differentiation medium was supplemented with 1 μg mL^{-1} of troglitazone and 0.25 mM isobutylmethylxanthine (IBMX) for the first 72 h. Fresh medium was provided every 2–3 d for up to 14 days.

2.6.2. RT-qPCR Analysis of Adipogenic Gene Expression

Quantitative RT-PCR analysis was performed to evaluate adipogenic marker expression at 7 and 14 d post-induction of differentiation ($n = 3$ samples per group per trial, $N = 3$ trials with different ASC donors) as per previously published protocols.[23] The TaqMan Gene Expression Assay human gene-specific primers conjugated with FAM-MGB probes (Invitrogen) used in this study were: peroxisome proliferator-activated receptor gamma (PPARγ, product code: Hs00234592_m1), lipoprotein lipase (LPL, product code: Hs00173425_m1), adiponectin (ADIPOQ, product code: Hs00605917_m1), and perilipin (PLIN1, product code: Hs00160173_m1), with glyceraldehyde-3-phosphate dehydrogenase (GAPDH, Product code: Hs02758991_g1) and Importin 8 (IPO8, Product code: Hs00183533_m1) used as the housekeeping genes. A comparative Ct method was used to calculate the relative fold change in gene expression relative to the uncoated TCP group at 7 d. No RT and no template controls were included on every plate.

2.6.3. Glycerol-3-Phosphate Dehydrogenase (GPDH) Activity

Intracellular GPDH enzyme activity was measured using a GPDH Activity Measurement Kit (Kamiya Biomedical Corporation, Cat. # KT-010, Seattle, WA, USA) at 7 and 14 d post-induction of adipogenic differentiation ($n = 3$ samples per group per trial, $N = 3$ trials with different ASC donors) using previously published methods.[30,37] For each cell donor, the data was normalized to the uncoated TCP group at 7 d for comparative purposes.

2.6.4. Immunocytochemical Assessment of Perilipin Expression

To qualitatively assess ASC adipogenesis, immunocytochemical analysis of perilipin expression was performed at 7 and 14 d post-induction of adipogenic differentiation ($n = 3$ wells per group per trial, $N = 2$ trials with different ASC donors). The coatings were fixed, rinsed, and blocked, as previously described. The samples were then incubated overnight at 4 °C with rabbit polyclonal anti-perilipin A (ab3526, Abcam, 1:200). Next, the samples were rinsed extensively with TBS and incubated with an Alexa Fluor 680 conjugated goat anti-rabbit IgG secondary antibody (ab175773, Abcam, 1:200) for 1 h at room temperature. Finally, the samples were rinsed in PBS and mounted with Fluoroshield with DAPI. Multiple nonoverlapping images were captured across the entire samples using an EVOS FL fluorescence imaging system.

2.7. Statistical Analysis

All numerical data are expressed as mean ± standard deviation (SD). All statistical analyses were performed using GraphPad Prism 6 (GraphPad Software, San Diego, CA) by two-way ANOVA with a Tukey's post-hoc comparison of the means. Differences were considered statistically significant at $p < 0.05$ unless otherwise noted.

3. Results

3.1. α-Amylase Digestion Generates Stable Coatings with a Fibrous Ultrastructure

The α-amylase-digested ECM suspensions appeared off-white, viscous, and cloudy, while pepsin digestion generated transparent yellow solutions with qualitatively lower viscosity (Figure S1a, Supporting Information). The 25 mg mL^{-1} ECM concentration was selected as it was the highest concentration of ECM that could be incorporated in the α-amylase-digested samples to produce a workable suspension that evenly coated the surface of the well plates. Molecular weight analysis by SDS-PAGE showed that α-amylase-digested ECM displayed distinct bands at a wide range of molecular weights (Figure S1c, Supporting Information), while the pepsin-digested ECM displayed only faint bands of smaller molecular weight.

Macroscopically, the α-amylase-digested ECM coatings were visually apparent and could be extracted from the TCP as intact sheets using forceps (Figure S1b, Supporting Information). Thickness measurements indicated that the α-amylase-digested DAT coatings were 160 ± 10 μm thick and the α-amylase-digested COL coatings were 150 ± 10 μm thick, providing a 3D microenvironment on a cellular scale. In contrast, the pepsin-digested coatings appeared as thin yellow films that could not be removed from the plastic. Based on SEM imaging, the α-amylase-digested ECM coatings had a multilayered fibrous ultrastructure, consistent with the preservation of high-molecular-weight collagen fibers (**Figure 1**A). Higher magnification analysis of these samples demonstrated the retained characteristic D-banding pattern of collagen (Figure S1d, Supporting Information). In contrast, the coatings generated with pepsin-digested ECM presented as thin films with no fibrous ultrastructure, consistent with the proteolytic degradation of the collagen fibers within the source materials.

Toluidine blue staining qualitatively supported that there was at least partial retention of the coatings after two rinses in proliferation medium (Figure 1B). Visualizing the α-amylase-digested samples was more challenging due to their nontransparent nature and thickness, but the staining was qualitatively similar for both ECM sources before and after rinsing. The hydroxyproline assay served as a quantitative measure of protein loss from the collagen-rich coatings during the rinses in proliferation medium (Figure 1C). Interestingly, there was significantly higher hydroxyproline content in the DAT samples relative to COL for both digestion methods, potentially attributed to the more complex ECM source. While no significant differences were noted in the hydroxyproline content before and after rinsing in the α-amylase-digested ECM coatings, a significant decrease in hydroxyproline content was observed for both the pepsin-digested ECM coatings following rinsing (Figure 1C).

Profilometry analyses corroborated the hydroxyproline data, with the thickness of the films generated with pepsin-digested DAT decreasing from 20 ± 4 μm to 4 ± 3 μm, and pepsin-digested COL decreasing from 15 ± 4 μm to 2 ± 1 μm following rinsing. Regional and sample variability indicated that coating retention was inconsistent across the samples. SEM images of the pepsin-digested thin films obtained after rinsing confirmed that coating materials
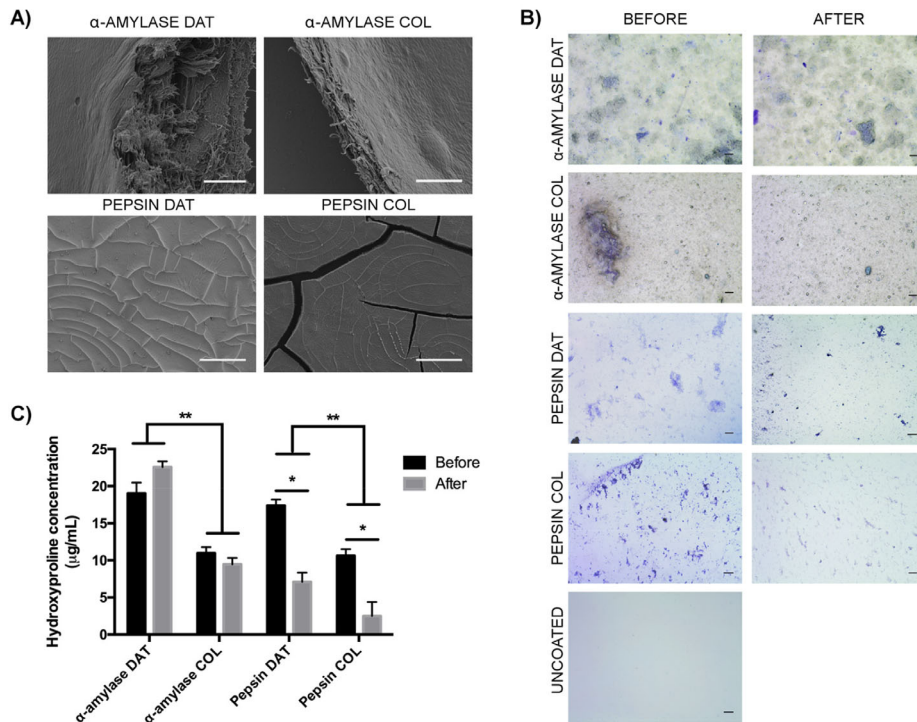
**ADVANCED
SCIENCE NEWS**
www.advancedsciencenews.com

**Biotechnology
Journal**
www.biotechnology-journal.com

Figure 1. A) SEM images of coating ultrastructure. The α-amylase-digested ECM coatings had a multilayered fibrous ultrastructure, while the pepsin-digested ECM coatings were macroscopically smooth thin films. Scale: 100 µm. B) Toluidine blue staining to qualitatively assess the coatings before and after two rinses in proliferation medium. The staining patterns relative to uncoated controls support that the coating materials remained on the TCP following rinsing in all of the groups. Scale: 10 µm. C) Quantitative assessment of coating stability via the hydroxyproline assay. There was significant protein loss from the pepsin-digested DAT and COL coatings following rinsing (*), while no change was observed in the α-amylase-digested samples. Further, the hydroxyproline content in the DAT samples was significantly higher than the COL samples for both digestion methods, both before and after rinsing. ($n = 3, *p < 0.01, **p < 0.0001$).

remained on the TCP prior to cell seeding (Figure S2, Supporting Information).

3.2. Coatings Generated with α-Amylase-Digested ECM Are Softer Than Those Generated with Pepsin-Digested ECM

AFM analysis of the α-amylase-digested fibrous coatings revealed an estimated Young's modulus of 36 ± 16 kPa for the DAT and 24 ± 10 kPa for the COL, respectively, with no significant differences between the two groups (**Figure 2**). The corresponding indentation depths were 180 ± 74 nm for the DAT coatings and 210 ± 47 nm for the COL coatings, which were both well below 10% of the sample thickness.[34] In contrast, the pepsin-digested coatings were substantially stiffer, with an estimated Young's modulus of 1060 ± 390 kPa for the DAT coatings and 505 ± 320 kPa for the COL coatings (Figure 2). The pepsin-digested thin films showed notable sample-to-sample and regional variability, potentially reflecting the reduced stability and variable protein loss seen in the previous rinse experiments. The corresponding indentation depths were 100 ± 7 nm for the DAT coatings and 129 ± 47 nm for the COL coatings, which were much closer to the range of 10% of the sample thickness.[34] Hence, the underlying substrate may have contributed in part to the measured values.
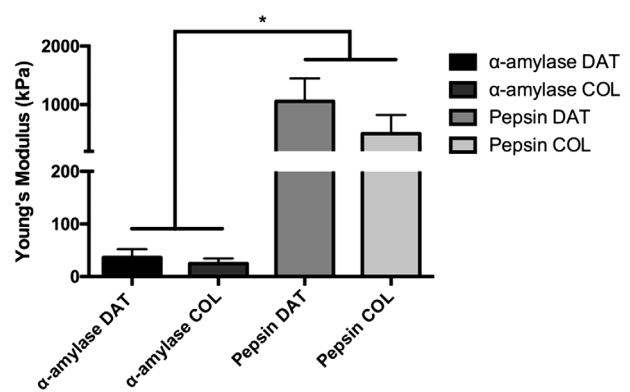

Figure 2. The coatings fabricated with α-amylase-digested ECM had significantly lower Young's moduli than the coatings fabricated with pepsin-digested ECM. No statistically significant differences were observed between the tissue sources for each digestion method ($n = 3$ for pepsin-digested coatings, $n = 6$ for α-amylase-digested coatings, $*p < 0.002$)

3.3. ASC Proliferation was Enhanced on the Coatings Fabricated with α-Amylase-Digested DAT

Based on DAPI quantification, the human ASCs readily attached to all substrates, with enhanced cell densities observed on the α-amylase-digested DAT coatings at all timepoints from 24 h to
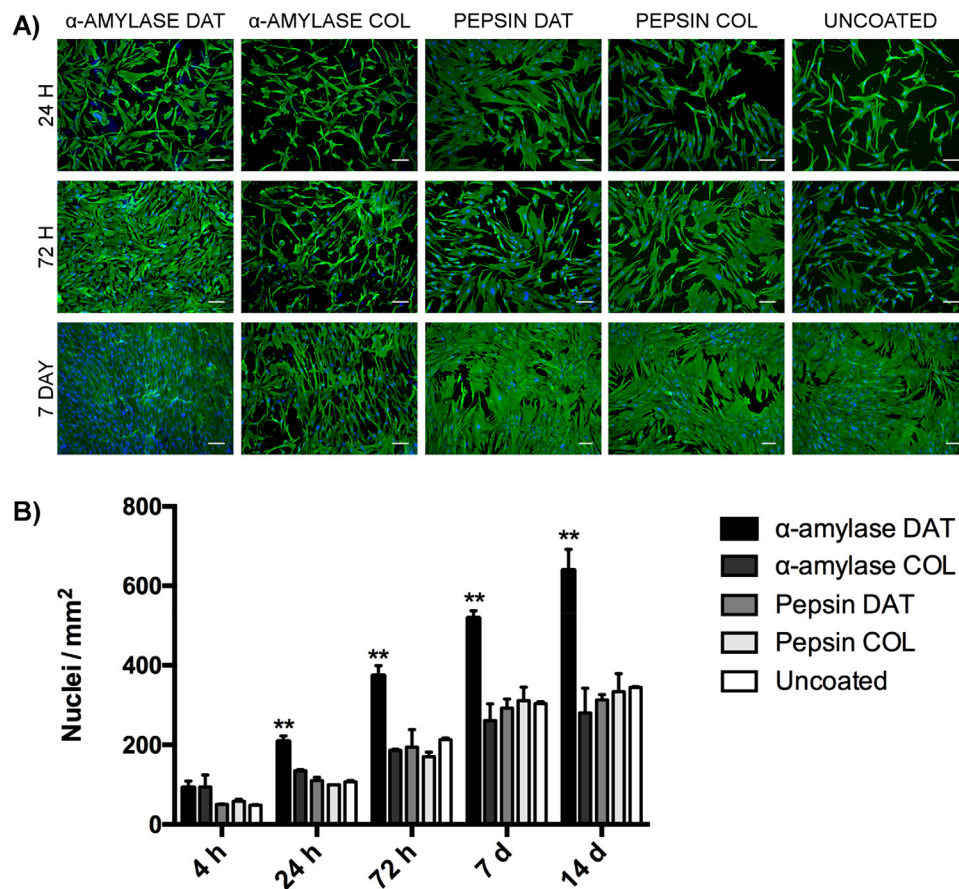
**ADVANCED
SCIENCE NEWS**
www.advancedsciencenews.com

**Biotechnology
Journal**
www.biotechnology-journal.com

Figure 3. Human ASCs cultured on α-amylase-digested DAT coatings showed enhanced proliferation and a more spindle-shaped morphology. A) Representative immunocytochemical staining for vimentin (green) with DAPI (blue) of ASCs cultured on the various substrates at 24 h, 72 h, and 7 d. Scale: 100 µm. B) Quantification of cell density over 14 d via DAPI nuclear counting. A significant increase in cell density was observed over the 14 d culture period for ASCs on the α-amylase-digested DAT coatings ($p < 0.0001$), with a significantly higher cell density observed at 24 h, 72 h, 7 d, and 14 d as compared to all other groups (**$p < 0.05$) (pooled results; $n = 3$ samples per group per trial, $N = 2$ trials with different ASC donors).

14 d relative to all other groups (**Figure 3**). Moreover, a significant increase in cell density was observed on the α-amylase-digested DAT group between each timepoint from 24 h to 14 d. In addition, staining for vimentin indicated that ASCs cultured on the fibrous coatings fabricated with α-amylase-digested ECM had a more spindle-shaped cellular morphology as compared to ASCs cultured on pepsin-digested ECM 2D coatings or uncoated controls, which showed greater cell spreading (Figure S3, Supporting Information).

3.4. Adipogenic Differentiation Is Enhanced in the ASCs Cultured on the Coatings Fabricated with α-Amylase-Digested DAT

Initial testing confirmed that P2 ASCs cultured on all substrates were successfully induced toward the adipogenic lineage through culture in the differentiation medium, with marked upregulation of the adipogenic genes and GPDH enzyme activity relative to non-induced cells by 7 days ($PPAR\gamma$ > 8-fold, LPL > 450-fold, $ADIPOQ$ > 4000-fold, $PLIN$ > 175-fold, GPDH activity > 20-fold for uncoated TCP), along with evidence of intracellular lipid

accumulation in all groups. To assess the pro-adipogenic capacity of the ECM-derived coatings, we focused our analysis on comparing the response on the various substrates relative to uncoated TCP under adipogenic conditions.

RT-qPCR analysis of adipogenic gene expression indicated that adipogenesis was enhanced in the ASCs cultured on the α-amylase-digested DAT coatings relative to all other groups (**Figure 4**A). While no difference was observed in the expression levels of the transcription factor $PPAR\gamma$, the expression of LPL, $ADIPOQ$, and $PLIN$ were enhanced in the α-amylase-digested DAT fibrous coatings as compared to all other substrates at both 7 and 14 d, with no significant changes in expression levels over time. Similarly, significantly higher GPDH enzyme activity was observed in the ASCs cultured on the α-amylase-digested DAT coatings as compared to all other groups at 7 d (Figure 4B). At 14 d, the GPDH activity levels were higher in the ASCs cultured on the α-amylase-digested DAT coatings relative to all other substrate conditions with the exception of the pepsin-digested DAT coatings. There were no significant differences in the GPDH activity levels between the two timepoints. Consistent with the gene and protein expression findings, immunocytochemical staining for perilipin (**Figure 5**) indicated that intracellular lipid
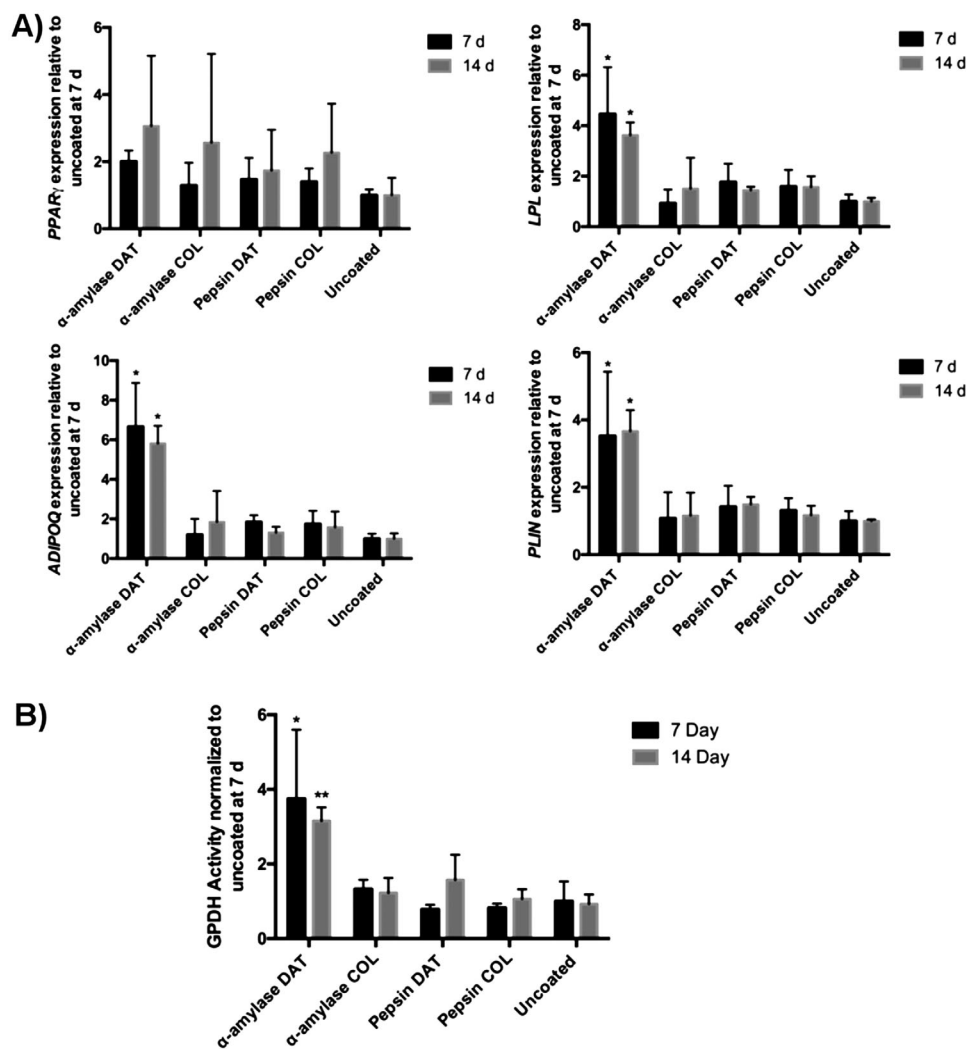
Figure 4. ASC adipogenic differentiation was enhanced on the α-amylase-digested DAT coatings. A) Adipogenic gene expression (*LPL*, *ADIPOQ*, and *PLIN*) was enhanced in the ASCs cultured on the α-amylase-digested DAT coatings. The data represents relative gene expression levels after 7 d and 14 d of culture in adipogenic differentiation medium, with *GAPDH* and *IPO8* as the housekeeping genes. (*$p < 0.05$) (Pooled results; $n = 3$ samples per group per trial, $N = 3$ trials with different ASC donors). B) GPDH enzyme activity levels were enhanced in human ASCs cultured on the α-amylase-digested DAT coatings relative to all other groups at 7 d (*) and relative to all other groups with the exception of the pepsin-digested DAT coatings at 14 d (**). (*, ** $p < 0.05$). (Pooled results; $n = 3$ samples per group per trial, $N = 3$ trials with different ASC donors).

accumulation was qualitatively enhanced in the ASCs cultured on the α-amylase-digested DAT coatings as compared to all other groups at both timepoints. Notably, there was a qualitative increase in perilipin expression in the α-amylase-digested DAT group from 7 to 14 d, with a uniform cellular response observed across the entire coating. The staining patterns were consistent with the progression toward a more mature phenotype associated with enhanced lipid accumulation and larger intracellular lipid droplets.

4. Discussion

There is a compelling need for cell culture models that more closely recapitulate the complex composition, structure, and biomechanics of the native extracellular milieu.[38] Recent studies have suggested that decellularized ECM-derived coatings can be harnessed to guide cell attachment and proliferation, as well as to promote the lineage-specific differentiation of stem cells in culture.[17,18,39,40] However, further research on the effects of enzymatic digestion on ECM bioactivity is warranted, as well as more systematic comparisons between ECM sources to assess the benefits of applying a tissue-specific approach.

In the present study, enzymatic digestion with α-amylase was investigated as an alternative approach to pepsin for generating ECM-derived coatings. In previous studies, our group has fabricated porous foams and microcarriers from α-amylase-digested human DAT,[23,24] porcine decellularized myocardium,[25] and porcine decellularized dermis.[22] However, to the best of our knowledge, this approach has not yet been applied to synthesize fibrous coatings. Our goal was to develop a more complex tissue-like microenvironment while retaining the convenience of
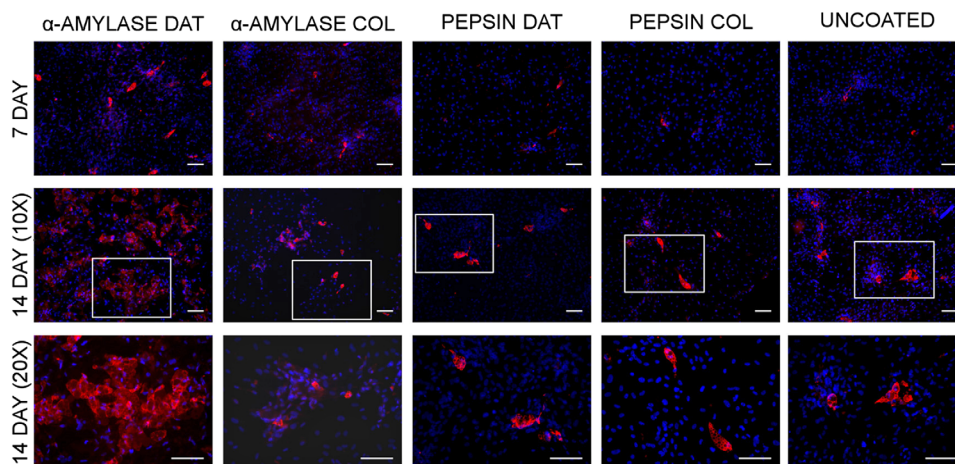
Figure 5. Intracellular lipid accumulation was enhanced in human ASCs cultured on the α-amylase-digested DAT coatings. Representative perilipin (red) staining with DAPI counterstaining (blue) of ASCs cultured on the various substrates in adipogenic differentiation medium for 7 d or 14 d. At 14 d, selected regions (white boxes) of the 10× images were visualized at higher magnification, as shown in the bottom row. Scale: 100 μm.

standard TCP formats and ability to perform characterization assays using the same methods applied with uncoated TCP. A secondary goal was to develop a deeper understanding of the potential benefits of applying adipose-derived ECM as a tissue-specific substrate for ASC expansion and adipogenic differentiation. Many studies assessing ECM-derived biomaterials lack appropriate tissue-type controls that are structurally and biomechanically similar, to be able to interpret whether there are tissue-specific compositional effects on the cells.[41] Hence, commercially sourced bovine tendon collagen served as a tissue-type control based on our previous studies characterizing the protein composition of this specific source,[42] as well as our previous success in applying α-amylase-digested COL to generate compositionally distinct porous foams relative to DAT.[32]

As expected, digestion with α-amylase better preserved the fibrillar structure of the ECM sources and retained a range of higher molecular weight proteins. Our findings are similar to a recent study that compared pepsin digestion, urea extraction, and homogenization in acetic acid as methods for generating coatings from decellularized ECM produced by placental mesenchymal stem/stromal cells (MSCs), which demonstrated that pepsin digestion produced clear solutions comprising low molecular weight (<50 kDa) proteins, while acetic acid homogenization generated the most complex mixture of proteins of varying sizes.[43] Interestingly, metabolic activity was enhanced on the pepsin-digested ECM coatings relative to the other groups, while coatings generated from urea extracts enhanced osteogenesis under differentiation conditions. Notably, the acetic-acid-homogenized ECM showed no bioactive effects relative to the uncoated TCP, which was postulated to be due to the heterogeneous nature of these coatings, as well as potentially the concentration employed (25 μg mL^{-1}).

Homogeneity and stability are important considerations when designing ECM coatings for use in long-term culture studies. From our analyses, the α-amylase-digested fibrous coatings were structurally robust and macroscopically homogeneous, with substantially greater thickness and enhanced stability compared to the pepsin-digested thin films. Rinsing twice in media reduced

the thickness and uniformity of the latter, suggesting that there may have been further protein loss over time in culture from these substrates, which may have contributed to the lack of observable bioactive effects in these groups. In contrast, the α-amylase-digested fibrous coatings were qualitatively retained over the 14 d culture studies, consistent with our previous work showing the long-term stability of microcarriers and foams generated with α-amylase-digested DAT.[23,24]

In addition to providing a more stable fibrous tissue-like environment, AFM analysis indicated that the α-amylase-digested coatings were significantly softer than the pepsin-digested thin films. The 5 μm spherical AFM tip enabled indentation testing over a larger region of the coatings, providing an analysis of the properties on the scale of individual cells. Notably, the α-amylase-digested DAT coatings were stiffer than the previous values measured through bulk compression testing for the intact DAT and α-amylase-digested DAT foams, which were in the range of ≈2–4 kPa and similar to the values reported for native human fat.[24,44] The increased stiffness of the coatings may be related to the difference in the scale of the testing methods employed, as well as structural differences in the materials and their processing to form coatings. The Young's moduli of the pepsin-digested thin films may have been impacted by the underlying glass substrate. However, previous studies have suggested that cells cultured on thin soft coatings (<10 μm) are able to sense the underlying stiff substrates.[45,46] Regardless of the actual gel stiffness, it would be expected that the pepsin-digested thin films would appear stiffer to the cells compared to the α-amylase-digested fibrous coatings. Notably, the similar structure and moduli between the α-amylase-digested DAT and COL suggests that the ECM composition was the predominant factor contributing to the enhanced proliferation and adipogenic differentiation of the human ASCs on the α-amylase-digested DAT.

A growing body of evidence indicates that strategies that avoid or minimize proteolytic digestion may be favorable for conserving bioactivity in ECM-derived substrates. A study comparing the bioactivity of solubilized decellularized cartilage and tendon ECM prepared through urea extraction versus pepsin digestion

**ADVANCED
SCIENCE NEWS**
www.advancedsciencenews.com

**Biotechnology
Journal**
www.biotechnology-journal.com

found that only the urea-extracted samples could promote the lineage-specific differentiation of human bone-marrow-derived MSCs.[16] Another study demonstrated that reducing pepsin digestion times enhanced the capacity of decellularized cardiac ECM coatings to promote cardiomyocyte proliferation, which was postulated to be due to changes in the composition of the substrates.[14] Building from this, we hypothesize that the enhanced proliferation on the α-amylase-digested DAT was due to the fibrous ultrastructure and more complex tissue-specific ECM composition of these substrates. Our findings are supported by other studies that have indicated that ECM coatings derived from other tissue sources can enhance cell attachment, survival, and proliferation in a tissue-specific manner.[16,39,40]

ASCs cultured on TCP are expected to have a spindle-shaped morphology, with cell spreading and flattening serving as markers of senescence in long-term culture.[47] In general, cell spreading varies in 2D and 3D systems, and correlates with properties such as substrate stiffness, ligand density, and arrangement through the regulation of focal adhesions.[45,48] As such, the spindle-shaped morphology observed on the α-amylase-digested coatings may be related to their lower stiffness and more fibrous 3D ultrastructure.[48] Fibrous topographies have been postulated to provide cells with a greater local surface area with multiple physical sites for engraftment in all three dimensions, favorable for cell attachment, migration, and proliferation.[49,50] Our findings are consistent with other studies that have shown that MSCs seeded on fibrous ECM-derived coatings were more elongated and had a more spindle-shaped morphology as compared to cells cultured on uncoated TCP or TCP coated with single ECM components (e.g., fibronectin).[51–53]

Consistent with previous studies of other DAT scaffold formats,[23,24,30,37] the current study demonstrates that adipose-derived ECM can provide a pro-adipogenic microenvironment for human ASCs. Enhanced differentiation was only observed on the α-amylase-digested DAT coatings, suggesting that the proteolytic digestion methods were unfavorable for conserving ECM bioactivity. In contrast to our findings, other groups have reported that hydrogels synthesized with pepsin-digested DAT can promote the adipogenic differentiation of human ASCs in culture and in vivo adipose tissue formation.[54,55] The differences in cellular response may be due to differences in scaffold composition and format (i.e., 2D vs 3D), which may impact properties including biomechanics, cell–ECM interactions, and substrate stability. Regardless, the new α-amylase-digested DAT fibrous coatings are highly promising for adipogenic cell culture studies. The uniform differentiation response on the α-amylase-digested DAT was noteworthy, with a much higher fraction of ASCs accumulating intracellular lipid and a more mature phenotype associated with larger intracellular lipid droplets.

The straightforward and scalable methods described enable the production of soft, compliant, and robust tissue-specific coatings that demonstrate cell-instructive effects. Despite the opaque nature of the α-amylase-digested substrates, which interferes with cell visualization using standard brightfield microscopy, the cells cultured on the coatings can be readily characterized using numerous standard biological assays including immunofluorescence, RT-PCR, and protein assays, supporting the utility of this platform for fundamental and applied cell biology research.

In conclusion, methods were developed for generating cell culture coatings using ECM digested with α-amylase in place of the standard proteolytic enzyme pepsin. The α-amylase-digested ECM was easily applied to produce soft, compliant, and stable cell-supportive substrates, with a 3D fibrillar ultrastructure and complex ECM composition. Notably, the coatings generated with α-amylase-digested DAT demonstrated tissue-specific cell-instructive effects, promoting human ASC proliferation and adipogenic differentiation. The α-amylase-digested DAT coatings combine the benefits of 3D culture with the ability to mimic native cell–ECM interactions, promote a high level of cell–cell contact favorable for adipogenesis, and the convenience of using standard assays for 2D systems. Overall, the α-amylase-digested DAT coatings may have broad utility as platforms for ASC expansion, as well as in tissue-specific culture models for applications in adipose tissue regeneration, obesity, diabetes, and metabolic research. The methods developed here could easily be extended to other decellularized tissue sources to create a wide-range of tissue-specific microenvironments that enable probing the effects of the ECM on cellular responses in the context of both health and disease.

Supporting Information

Supporting Information is available from the Wiley Online Library or from the author.

Conflict of Interest

The authors declare no conflict of interest.

[1] M. van Dijk, S. A. Göransson, S. Strömblad, *Exp. Cell Res.* **2013**, *319*, 1663.

[2] F. Gattazzo, A. Urciuolo, P. Bonaldo, *Biochim. Biophys. Acta, Gen. Subj.* **2014**, *1840*, 2506.

[3] C. McKee, G. R. Chaudhry, *Colloids Surf., B* **2017**, *159*, 62.

[4] K. Duval, H. Grover, L.-H. Han, Y. Mou, A. F. Pegoraro, J. Fredberg, Z. Chen, *Physiology* **2017**, *32*, 266. https://doi.org/10.1152/physiol.00036.2016

[5] M. P. Lutolf, P. M. Gilbert, H. M. Blau, *Nature* **2009**, *462*, 433.

[6] S. Heydarkhan-Hagvall, J. M. Gluck, C. Delman, M. Jung, N. Ehsani, S. Full, R. J. Shemin, *Biomaterials* **2012**, *33*, 2032.

[7] C. Somaiah, A. Kumar, D. Mawrie, A. Sharma, *PLoS One* **2015**, *10*, e0145068.

[8] A. Kasten, T. Naser, K. Brüllhoff, J. Fiedler, P. Müller, M. Möller, J. Rychly, J. Groll, R. E. Brenner, *PLoS One* **2014**, *9*, e109411.

[9] S. Schwarz, L. Koerber, A. F. Elsaesser, E. Goldberg-Bockhorn, A. M. Seitz, L. Dürselen, A. Ignatius, P. Walther, R. Breiter, N. Rotter, *Tissue Eng., Part A* **2012**, *18*, 2195.

[10] D. J. Lee, S. Diachina, Y. T. Lee, L. Zhao, R. Zou, N. Tang, H. Han, X. Chen, C.-C. Ko, *J. Tissue Eng.* **2016**, *7*, 2041731416668030.

[11] Z. Wu, Y. Tang, H. Fang, Z. Su, B. Xu, Y. Lin, P. Zhang, X. Wei, *J. Mater. Sci. Mater. Med.* **2015**, *26*, 5322.

[12] F. Pati, J. Jang, D.-H. Ha, S. Won Kim, J.-W. Rhie, J.-H. Shim, D.-H. Kim, D.-W. Cho, *Nat. Commun.* **2014**, *5*, 3935.

[13] L. E. Flynn, *Biomaterials* **2010**, *31*, 4715.

[14] C. Williams, K. Sullivan, L. D. Black, *Adv. Healthcare Mater.* **2015**, *4*, 1545.

[15] J. A. Dequach, V. Mezzano, A. Miglani, S. Lange, G. M. Keller, K. L. Christman, *PLoS One* **2010**, *5*, e13039.

[16] B. B. Rothrauff, G. Yang, R. S. Tuan, *Stem Cell Res. Ther.* **2017**, *8*, 133.

[17] J. S. Lee, J. Shin, H. M. Park, Y. G. Kim, B. G. Kim, J. W. Oh, S. W. Cho, *Biomacromolecules* **2014**, *15*, 206.

[18] J. A. DeQuach, S. H. Yuan, L. S. B. Goldstein, K. L. Christman, *Tissue Eng., Part A* **2011**, *17*, 2583.

[19] H. Lin, G. Yang, J. Tan, R. S. Tuan, *Biomaterials* **2012**, *33*, 4480.

[20] A. E. B. Turner, L. E. Flynn, *Tissue Eng., Part C* **2012**, *18*, 186.

[21] J. Visser, P. A. Levett, N. C. R. te Moller, J. Besems, K. W. M. Boere, M. H. P. van Rijen, J. C. de Grauw, W. J. A. Dhert, P. R. van Weeren, J. Malda, *Tissue Eng., Part A* **2015**, *21*, 1195.

[22] A. Kornmuller, C. F. C. Brown, C. Yu, L. E. Flynn, *J. Vis. Exp.* **2017**, e55436.

[23] C. Yu, A. Kornmuller, C. Brown, T. Hoare, L. E. Flynn, *Biomaterials* **2017**, *120*, 66.

[24] C. Yu, J. Bianco, C. Brown, L. Fuetterer, J. F. Watkins, A. Samani, L. E. Flynn, *Biomaterials* **2013**, *34*, 3290.

[25] V. Russo, E. Omidi, A. Samani, A. Hamilton, L. E. Flynn, *BioRes. Open Access* **2015**, *4*, 374.

[26] G. Quintarelli, C. Dellovo, C. Balduini, A. A. Castellani, *Histochemie.* **1969**, *18*, 373.

[27] F. S. Steven, *Ann. Rheum. Dis.* **1964**, *23*, 300.

[28] L. Flynn, J. L. Semple, K. A. Woodhouse, *J. Biomed. Mater. Res., Part A*, **2006**, *79A*, 359.

[29] V. Russo, C. Yu, P. Belliveau, A. Hamilton, L. E. Flynn, *Stem Cells Transl. Med.* **2014**, *3*, 206.

[30] C. F. C. Brown, J. Yan, T. T. Y. Han, D. M. Marecak, B. G. Amsden, L. E. Flynn, *Biomed. Mater.* **2015**, *10*, 045010.

[31] S. B. Seif-Naraghi, M. A. Salvatore, P. J. Schup-Magoffin, D. P. Hu, K. L. Christman, *Tissue Eng., Part A* **2010**, *16*, 2017.

[32] P. M. Martin, A. Grant, D. W. Hamilton, L. E. Flynn, *Acta Biomater.* **2019**, *83*, 199.

[33] H. Liu, Y. Sun, C. A. Simmons, *J. Biomech.* **2013**, *46*, 1967.

[34] H. Bückle, *Metall. Rev.* **1959**, *4*, 49.

[35] I. Manika, J. Maniks, *J. Phys. D: Appl. Phys.* **2008**, *41*, 6, https://doi.org/10.1088/0022-3727/41/7/074010.

[36] H. Hauner, T. Skurk, M. Wabitsch, *Methods Mol. Biol.* **2001**, *155*, 239.

[37] H. Ki, T. Tian, Y. Han, D. M. Marecak, J. F. Watkins, B. G. Amsden, L. E. Flynn, *Biomaterials* **2014**, *35*, 9668.

[38] E. Knight, S. Przyborski, *J. Anat.* **2015**, *227*, 746.

[39] Y. Zhang, Y. He, S. Bharadwaj, N. Hammam, K. Carnagey, R. Myers, A. Atala, M. Van Dyke, *Biomaterials* **2009**, *30*, 4021.

[40] M. M. Stern, R. L. Myers, N. Hammam, K. A. Stern, D. Eberli, S. B. Kritchevsky, S. Soker, M. Van Dyke, *Biomaterials* **2009**, *30*, 2393.

[41] K. P. Robb, A. Shridhar, L. E. Flynn, *ACS Biomater. Sci. Eng.* **2017**, *4*, 3627.

[42] M. Kuljanin, C. F. C. Brown, M. J. Raleigh, G. A. Lajoie, L. E. Flynn, *Biomaterials* **2017**, *144*, 130.

[43] G. D. Kusuma, M. C. Yang, S. P. Brennecke, A. J. O'Connor, B. Kalionis, D. E. Heath, *ACS Biomater. Sci. Eng.* **2018**, *4*, 1760.

[44] E. Omidi, L. Fuetterer, S. Reza Mousavi, R. C. Armstrong, L. E. Flynn, A. Samani, *J. Biomech.* **2014**, *47*, 3657.

[45] C. A. Mullen, T. J. Vaughan, K. L. Billiar, L. M. McNamara, *Biophys. J.* **2015**, *108*, 1604.

[46] S. Sen, A. J. Engler, D. E. Discher, *Cell Mol. Bioeng.* **2009**, *2*, 39.

[47] D. Legzdina, A. Romanauska, S. Nikulshin, T. Kozlovska, U. Berzins, *Int. J. Stem Cells* **2016**, *9*, 124.

[48] C. G. Tusan, Y.-H. Man, H. Zarkoob, D. A. Johnston, O. G. Andriotis, P. J. Thurner, S. Yang, E. A. Sander, E. Gentleman, B. G. Sengers, N. D. Evans, *Biophys. J.* **2018**, *114*, 2743.

[49] B. M. Baker, B. Trappmann, W. Y. Wang, M. S. Sakar, I. L. Kim, V. B. Shenoy, J. A. Burdick, C. S. Chen, *Nat. Mater.* **2015**, *14*, 1262.

[50] X. Li, R. You, Z. Luo, G. Chen, M. Li, *J. Mater. Chem. B* **2016**, *4*, 2903.

[51] M. Pei, F. He, V. L. Kish, *Tissue Eng., Part A* **2011**, *17*, 3067.

[52] R. Rakian, T. J. Block, S. M. Johnson, M. Marinkovic, J. Wu, Q. Dai, D. D. Dean, X.-D. Chen, *Stem Cell Res. Ther.* **2015**, *6*, 235.

[53] C. P. Ng, A. R. M. Sharif, D. E. Heath, J. W. Chow, C. B. Zhang, M. B. Chan-Park, P. T. Hammond, J. K. Chan, L. G. Griffith, *Biomaterials* **2014**, *35*, 4046.

[54] D. A. Young, V. Bajaj, K. L. Christman, *J. Biomed. Mater. Res., Part A* **2014**, *102*, 1641.

[55] B. N. Brown, J. M. Freund, L. Han, J. P. Rubin, J. E. Reing, E. M. Jeffries, M. T. Wolf, S. Tottey, C. A. Barnes, B. D. Ratner, S. F. Badylak, *Tissue Eng., Part C* **2011**, *17*, 411.